

# Results on neutrinoless double beta decay of $^{76}\text{Ge}$ from GERDA Phase I

M. Agostini,<sup>14</sup> M. Allardt,<sup>3</sup> E. Andreotti,<sup>17,5</sup> A.M. Bakalyarov,<sup>12</sup> M. Balata,<sup>1</sup> I. Barabanov,<sup>10</sup> M. Barnabé Heider,<sup>6,14,a</sup> N. Barros,<sup>3</sup> L. Baudis,<sup>18</sup> C. Bauer,<sup>6</sup> N. Becerici-Schmidt,<sup>13</sup> E. Bellotti,<sup>7,8</sup> S. Belogurov,<sup>11,10</sup> S.T. Belyaev,<sup>12</sup> G. Benato,<sup>18</sup> A. Bettini,<sup>15,16</sup> L. Bezrukov,<sup>10</sup> T. Bode,<sup>14</sup> V. Brudanin,<sup>4</sup> R. Brugnera,<sup>15,16</sup> D. Budjáš,<sup>14</sup> A. Caldwell,<sup>13</sup> C. Cattadori,<sup>8</sup> A. Chernogorov,<sup>11</sup> F. Cossavella,<sup>13</sup> E.V. Demidova,<sup>11</sup> A. Domula,<sup>3</sup> V. Egorov,<sup>4</sup> R. Falkenstein,<sup>17</sup> A. Ferella,<sup>18,b</sup> K. Freund,<sup>17</sup> N. Frodyma,<sup>2</sup> A. Gangapshev,<sup>10,6</sup> A. Garfagnini,<sup>15,16</sup> C. Gotti,<sup>8,c</sup> P. Grabmayr,<sup>17</sup> V. Gurentsov,<sup>10</sup> K. Gusev,<sup>12,4,14</sup> K.K. Guthikonda,<sup>18</sup> W. Hampel,<sup>6</sup> A. Hegai,<sup>17</sup> M. Heisel,<sup>6</sup> S. Hemmer,<sup>15,16</sup> G. Heusser,<sup>6</sup> W. Hofmann,<sup>6</sup> M. Hult,<sup>5</sup> L.V. Inzhechik,<sup>10,d</sup> L. Ioannucci,<sup>1</sup> J. Janicskó Csáthy,<sup>14</sup> J. Jochum,<sup>17</sup> M. Junker,<sup>1</sup> T. Kihm,<sup>6</sup> I.V. Kirpichnikov,<sup>11</sup> A. Kirsch,<sup>6</sup> A. Klimenko,<sup>4,6,e</sup> K.T. Knöpfle,<sup>6</sup> O. Kochetov,<sup>4</sup> V.N. Kornoukhov,<sup>11,10</sup> V.V. Kuzminov,<sup>10</sup> M. Laubenstein,<sup>1</sup> A. Lazzaro,<sup>14</sup> V.I. Lebedev,<sup>12</sup> B. Lehnert,<sup>3</sup> H.Y. Liao,<sup>13</sup> M. Lindner,<sup>6</sup> I. Lippi,<sup>16</sup> X. Liu,<sup>13,f</sup> A. Lubashevskiy,<sup>6</sup> B. Lubsandorzhiev,<sup>10</sup> G. Lutter,<sup>5</sup> C. Macolino,<sup>1</sup> A.A. Machado,<sup>6</sup> B. Majorovits,<sup>13</sup> W. Maneschg,<sup>6</sup> M. Misiaszek,<sup>2</sup> I. Nemchenok,<sup>4</sup> S. Nisi,<sup>1</sup> C. O'Shaughnessy,<sup>13,g</sup> L. Pandola,<sup>1</sup> K. Pelczar,<sup>2</sup> G. Pessina,<sup>8,7</sup> A. Pullia,<sup>9</sup> S. Riboldi,<sup>9</sup> N. Rumyantseva,<sup>4</sup> C. Sada,<sup>15,16</sup> M. Salathe,<sup>6</sup> C. Schmitt,<sup>17</sup> J. Schreiner,<sup>6</sup> O. Schulz,<sup>13</sup> B. Schwingenheuer,<sup>6</sup> S. Schönert,<sup>14</sup> E. Shevchik,<sup>4</sup> M. Shirchenko,<sup>12,4</sup> H. Simgen,<sup>6</sup> A. Smolnikov,<sup>6</sup> L. Stanco,<sup>16</sup> H. Strecker,<sup>6</sup> M. Tarka,<sup>18</sup> C.A. Ur,<sup>16</sup> A.A. Vasenko,<sup>11</sup> O. Volynets,<sup>13</sup> K. von Sturm,<sup>15,16</sup> V. Wagner,<sup>6</sup> M. Walter,<sup>18</sup> A. Wegmann,<sup>6</sup> T. Wester,<sup>3</sup> M. Wojcik,<sup>2</sup> E. Yanovich,<sup>10</sup> P. Zavarise,<sup>1,h</sup> I. Zhitnikov,<sup>4</sup> S.V. Zhukov,<sup>12</sup> D. Zinatulina,<sup>4</sup> K. Zuber,<sup>3</sup> and G. Zuzel<sup>2</sup>  
(GERDA collaboration)<sup>i</sup>

<sup>1</sup>INFN Laboratori Nazionali del Gran Sasso, LNGS, Assergi, Italy

<sup>2</sup>Institute of Physics, Jagiellonian University, Cracow, Poland

<sup>3</sup>Institut für Kern- und Teilchenphysik, Technische Universität Dresden, Dresden, Germany

<sup>4</sup>Joint Institute for Nuclear Research, Dubna, Russia

<sup>5</sup>Institute for Reference Materials and Measurements, Geel, Belgium

<sup>6</sup>Max-Planck-Institut für Kernphysik, Heidelberg, Germany

<sup>7</sup>Dipartimento di Fisica, Università Milano Bicocca, Milano, Italy

<sup>8</sup>INFN Milano Bicocca, Milano, Italy

<sup>9</sup>Dipartimento di Fisica, Università degli Studi di Milano e INFN Milano, Milano, Italy

<sup>10</sup>Institute for Nuclear Research of the Russian Academy of Sciences, Moscow, Russia

<sup>11</sup>Institute for Theoretical and Experimental Physics, Moscow, Russia

<sup>12</sup>National Research Centre "Kurchatov Institute", Moscow, Russia

<sup>13</sup>Max-Planck-Institut für Physik, München, Germany

<sup>14</sup>Physik Department and Excellence Cluster Universe, Technische Universität München, München, Germany

<sup>15</sup>Dipartimento di Fisica e Astronomia dell'Università di Padova, Padova, Italy

<sup>16</sup>INFN Padova, Padova, Italy

<sup>17</sup>Physikalisches Institut, Eberhard Karls Universität Tübingen, Tübingen, Germany

<sup>18</sup>Physik Institut der Universität Zürich, Zürich, Switzerland

(Dated: February 25, 2022)

Neutrinoless double beta decay is a process that violates lepton number conservation. It is predicted to occur in extensions of the Standard Model of particle physics. This Letter reports the results from Phase I of the GERmanium Detector Array (GERDA) experiment at the Gran Sasso Laboratory (Italy) searching for neutrinoless double beta decay of the isotope  $^{76}\text{Ge}$ . Data considered in the present analysis have been collected between November 2011 and May 2013 with a total exposure of 21.6 kg·yr. A blind analysis is performed. The background index is about  $1 \cdot 10^{-2}$  cts/(keV·kg·yr) after pulse shape discrimination. No signal is observed and a lower limit is derived for the half-life of neutrinoless double beta decay of  $^{76}\text{Ge}$ ,  $T_{1/2}^{0\nu} > 2.1 \cdot 10^{25}$  yr (90 % C.L.). The combination with the results from the previous experiments with  $^{76}\text{Ge}$  yields  $T_{1/2}^{0\nu} > 3.0 \cdot 10^{25}$  yr (90 % C.L.).

PACS numbers: 23.40.-s, 21.10.Tg, 27.50.+e, 29.40.Wk

Keywords: neutrinoless double beta decay,  $T_{1/2}^{0\nu}$ ,  $^{76}\text{Ge}$ , enriched Ge detectors

## INTRODUCTION

For several isotopes beta decay is energetically forbidden but the simultaneous occurrence of two beta

decays ( $2\nu\beta\beta$ ) is allowed. This process has been observed in eleven nuclei with half-lives in the range of  $10^{18} - 10^{24}$  yr [1, 2]. Extensions of the Standard Model predict that also neutrinoless double beta ( $0\nu\beta\beta$ ) decay should exist:  $(A,Z) \rightarrow (A,Z+2) + 2e^-$ . In this process lep-

ton number is violated by two units and the observation would have far-reaching consequences [3–6]. It would prove that neutrinos have a Majorana mass component. Assuming the exchange of light Majorana neutrinos, an effective neutrino mass can be evaluated by using predictions for the nuclear matrix element (NME).

The experimental signature of  $0\nu\beta\beta$  decay is a peak at the  $Q$ -value of the decay. The two most sensitive experiments with the candidate nucleus  $^{76}\text{Ge}$  ( $Q_{\beta\beta} = 2039.061 \pm 0.007$  keV [7]) were Heidelberg-Moscow (HDM) [8] and the International GERmanium eXperiment (IGEX) [9, 10]. They found no evidence for the  $0\nu\beta\beta$  decay of  $^{76}\text{Ge}$  and set lower limits on the half-life  $T_{1/2}^{0\nu} > 1.9 \cdot 10^{25}$  yr and  $> 1.6 \cdot 10^{25}$  yr at 90 % C.L., respectively. Part of HDM published a claim to have observed  $(28.75 \pm 6.86)$   $0\nu\beta\beta$  decays [11] and reported  $T_{1/2}^{0\nu} = (1.19_{-0.23}^{+0.37}) \cdot 10^{25}$  yr. Later, pulse shape information was used to strengthen the claim [12]. Because of inconsistencies in the latter reference pointed out recently [13], the present comparison is restricted to the result of Ref. [11].

Until recently, the claim has not been scrutinized. The currently most sensitive experiments are KamLAND-Zen [14] and EXO-200 [15] looking for  $0\nu\beta\beta$  decay of  $^{136}\text{Xe}$  and GERDA [16] employing  $^{76}\text{Ge}$ . Nuclear matrix element calculations are needed to relate the different isotopes. Thus the experiments using  $^{136}\text{Xe}$  can not refute the claim in a model-independent way. GERDA is able to perform a direct test using the same isotope and also using mostly the same detectors as HDM and IGEX. This paper reports the  $0\nu\beta\beta$  results of Phase I of GERDA.

## THE EXPERIMENT

The GERDA experiment [16] is located at the Laboratori Nazionali del Gran Sasso (LNGS) of INFN in Italy. High-purity germanium (HPGe) detectors made from isotopically modified material with  $^{76}\text{Ge}$  enriched to  $\sim 86$  % ( $^{\text{enr}}\text{Ge}$ ) are mounted in low-mass copper supports and immersed in a  $64 \text{ m}^3$  cryostat filled with liquid argon (LAr). The LAr serves as cooling medium and shield against external backgrounds. The shielding is complemented by 3 m of water which is instrumented with photo multipliers to detect Cherenkov light generated by muons. The HPGe detector signals are read out with custom-made charge sensitive amplifiers optimized for low radioactivity which are operated close to the detectors in LAr. The analog signals are digitized with 100 MHz Flash ADCs and analyzed offline. If one of the detectors has an energy deposition above the trigger threshold (40–100 keV), all channels are analyzed for possible coincidences.

Reprocessed  $p$ -type semi-coaxial detectors from the HDM and IGEX experiments were operated together with newly produced GERDA Phase II detectors. The latter are of BEGe type manufactured by Canberra [17]. The

active volume fraction  $f_{av}$  of the detectors was determined beforehand amounting to 0.87 (0.92) for the semi-coaxial (BEGe) detectors [16, 18].

Data acquisition started in November 2011 with eight  $^{\text{enr}}\text{Ge}$  detectors (ANG 1-5 from HDM and RG 1-3 from IGEX), totaling a weight of 17.67 kg. Five enriched GERDA Phase II detectors of 3.63 kg in total were deployed in July 2012. ANG 1 and RG 3 started to draw leakage current soon after their deployment, and are omitted in this analysis. One BEGe detector showed an unstable behavior and is omitted as well. Since March 2013, RG 2 is no longer used since it is operated below its full depletion voltage. A fraction of 5 % of the data was discarded because of temperature-related instabilities. Results from the data collected until May 2013 (492.3 live days) are reported here. The total exposure considered for the analysis amounts to  $21.6 \text{ kg}\cdot\text{yr}$  of  $^{\text{enr}}\text{Ge}$  detector mass, yielding  $(215.2 \pm 7.6) \text{ mol}\cdot\text{yr}$  of  $^{76}\text{Ge}$  within the active volume.

The offline analysis of the digitized charge pulses is performed with the software tool GELATIO [19] and the procedure described in Ref. [20]. The deposited energy is reconstructed by a digital filter with semi-Gaussian shaping. Events generated by discharges or due to electromagnetic noise are rejected by a set of quality cuts.

The energy scale of the individual detectors is determined with  $^{228}\text{Th}$  sources once every one or two weeks. The differences between the reconstructed peak positions and the ones from the calibration curves are smaller than 0.3 keV. The energy resolution was stable over the entire data acquisition period. The gain variation between consecutive calibrations is less than 0.05 % [16], which corresponds to  $< 30$  % of the expected energy resolution (Full Width Half Maximum, FWHM) at  $Q_{\beta\beta}$ . Between calibrations, the stability is monitored by regularly injecting charge pulses into the input of the amplifiers.

The energy spectrum and its decomposition into individual sources is discussed in Ref. [18]. Peaks from  $^{40}\text{K}$ ,  $^{42}\text{K}$ ,  $^{214}\text{Bi}$ ,  $^{214}\text{Pb}$  and  $^{208}\text{Tl}$   $\gamma$  rays can be identified as well as  $\alpha$  decays from the  $^{226}\text{Ra}$  decay chain, and  $\beta$  events from  $^{39}\text{Ar}$ . All  $\gamma$ -ray peaks are reconstructed at the correct energy within their statistical uncertainty. The energy resolution (FWHM) of the strongest line (1524.6 keV from  $^{42}\text{K}$ ) is 4.5 (3.1) keV for the semi-coaxial (BEGe) detectors. These values are about 10 % larger than the resolutions obtained from calibrations. The broadening is due to fluctuations of the energy scale between calibrations. The interpolated FWHM at  $Q_{\beta\beta}$  for physics data is detector dependent and varies between 4.2 and 5.7 keV for the semi-coaxial detectors, and between 2.6 and 4.0 keV for the BEGe detectors. The exposure-averaged values are  $(4.8 \pm 0.2)$  keV and  $(3.2 \pm 0.2)$  keV, respectively.

For the first time in the field of  $0\nu\beta\beta$  decay search, a blind analysis was performed in order to avoid bias in the event selection criteria. Events with energies within

$Q_{\beta\beta} \pm 20$  keV were not processed. After the energy calibration and the background model were finalized the window was opened except for  $\pm 5$  keV ( $\pm 4$  keV) around  $Q_{\beta\beta}$  for the semi-coaxial (BEGe) detectors. After all selections discussed below had been frozen, the data in the  $Q_{\beta\beta}$  region were analyzed. The validity of the offline energy reconstruction and of the event selection procedures have been cross-checked with a fully independent analysis.

### $0\nu\beta\beta$ ANALYSIS

The signature for  $0\nu\beta\beta$  decay is a single peak at  $Q_{\beta\beta}$ . Furthermore, events from  $0\nu\beta\beta$  decays have a distinct topology, which allows to distinguish them from  $\gamma$ -induced background. For  $0\nu\beta\beta$  events, energy is deposited by the two electrons, which have a short range in germanium: more than 90 % of  $0\nu\beta\beta$  events are expected to deposit all energy localized within few mm<sup>3</sup> (single-site events, SSE). On the other hand, most background events from  $\gamma$ -ray interactions have energy depositions in many detectors or at different, well separated, positions (multi-site events, MSE).

Only events with an energy deposition in a single detector are accepted resulting in a background reduction by about 15 % around  $Q_{\beta\beta}$ , with no efficiency loss for  $0\nu\beta\beta$  decays. Events in the HPGe detectors are rejected if they are in coincidence within 8  $\mu$ s with a signal from the muon veto. This leads to a further background reduction by about 7 %. Events which are preceded or followed by another event in the same detector within 1 ms are excluded. This allows to reject background events from the  $^{214}\text{Bi}$ - $^{214}\text{Po}$  cascade (BiPo) in the  $^{222}\text{Rn}$  decay chain. Less than 1 % of the events at  $Q_{\beta\beta}$  are affected by this cut. Due to the low counting rate in GERDA and due to the low muon flux at LNGS, the dead time due to the muon veto and BiPo cuts is negligible.

The detector signals are different for SSE and MSE, and also surface events from  $\beta$  or  $\alpha$  decays exhibit a characteristic shape. Thus, pulse shape discrimination (PSD) techniques can improve the sensitivity.

For BEGe detectors, a simple and effective PSD is based on the ratio of the maximum of the current pulse (called  $A$ ) over the energy  $E$  [21–23]. The  $A/E$  cut efficiency is determined from calibration data using events in the double escape peak (DEP) of the 2615 keV  $\gamma$  ray from  $^{208}\text{Tl}$ . It is cross-checked with  $2\nu\beta\beta$  decays of  $^{76}\text{Ge}$ . The acceptance of signal events at  $Q_{\beta\beta}$  is  $\varepsilon_{psd} = 0.92 \pm 0.02$ , while only 20 % of the background events at this energy survive.

For the semi-coaxial detectors, a PSD method based on an artificial neural network (ANN) [23] is used. The signal acceptance  $\varepsilon_{psd} = 0.90^{+0.05}_{-0.09}$  is adjusted with DEP events and the uncertainty is derived from the  $2\nu\beta\beta$  spectrum and from events at the Compton edge. About 55 %

of the background events around  $Q_{\beta\beta}$  are classified as SSE-like and considered for the analysis. Two alternative PSD methods were developed based on a likelihood ratio and on a combination of  $A/E$  and the asymmetry of the current pulse; they are used for cross-checks. The three PSD methods use very different training samples and selection criteria but more than 90 % of the events rejected by ANN are also rejected by the two other algorithms.

The half-life on  $0\nu\beta\beta$  decay is calculated as

$$T_{1/2}^{0\nu} = \frac{\ln 2 \cdot N_A}{m_{enr} \cdot N^{0\nu}} \cdot \mathcal{E} \cdot \epsilon \quad (1)$$

$$\epsilon = f_{76} \cdot f_{av} \cdot \varepsilon_{fep} \cdot \varepsilon_{psd} \quad (2)$$

with  $N_A$  being Avogadro's constant,  $\mathcal{E}$  the total exposure (detector mass  $\cdot$  live time), and  $m_{enr} = 75.6$  g the molar mass of the enriched material.  $N^{0\nu}$  is the observed signal strength or the corresponding upper limit. The efficiency  $\epsilon$  accounts for the fraction of  $^{76}\text{Ge}$  atoms ( $f_{76}$ ), the active volume fraction ( $f_{av}$ ), the signal acceptance by PSD ( $\varepsilon_{psd}$ ), and  $\varepsilon_{fep}$ . The latter is the probability that a  $0\nu\beta\beta$  decay taking place in the active volume of a detector releases its entire energy in it, contributing to the full energy peak at  $Q_{\beta\beta}$ . Energy losses are due to bremsstrahlung photons, fluorescence X-rays, or electrons escaping the detector active volume. Monte Carlo simulations yield  $\varepsilon_{fep} = 0.92$  (0.90) for semi-coaxial (BEGe) detectors.

The GERDA background model [18] predicts approximately a flat energy distribution between 1930 and 2190 keV from Compton events of  $\gamma$  rays of  $^{208}\text{Tl}$  and  $^{214}\text{Bi}$  decays, degraded  $\alpha$  events, and  $\beta$  rays from  $^{42}\text{K}$  and  $^{214}\text{Bi}$ . The signal region ( $2039 \pm 5$ ) keV and the intervals ( $2104 \pm 5$ ) keV and ( $2119 \pm 5$ ) keV, which contain known  $\gamma$ -ray peaks from  $^{208}\text{Tl}$  and  $^{214}\text{Bi}$ , respectively, are excluded in the background calculation. The net width of the window used for the evaluation of the constant background is hence 230 keV.

Data are grouped into three subsets with similar characteristics: (i) data from the BEGe detectors form one set, (ii) the *golden* data set contains the major part of the data from the semi-coaxial detectors except (iii) two short periods with higher background levels when the BEGe detectors were inserted (*silver* data set).

## RESULTS

Table I lists the observed number of events in the interval  $Q_{\beta\beta} \pm 5$  keV for the three data sets, the number of background events in the 230 keV window and the exposure-weighted average efficiency  $\langle \epsilon \rangle$  over all detectors. Table II reports the details of these events including the results from the PSD analysis. The combined energy spectrum around  $Q_{\beta\beta}$ , with and without the PSD selection, is displayed in Fig. 1.

TABLE I. Parameters for the three data sets with and without the pulse shape discrimination (PSD). “bkg” is the number of events in the 230 keV window and BI the respective background index, calculated as  $\text{bkg}/(\mathcal{E} \cdot 230 \text{ keV})$ . “cts” is the observed number of events in the interval  $Q_{\beta\beta} \pm 5 \text{ keV}$ .

data set	$\mathcal{E}[\text{kg}\cdot\text{yr}]$	$\langle\epsilon\rangle$	bkg	BI <sup>†</sup>	cts
without PSD					
<i>golden</i>	17.9	$0.688 \pm 0.031$	76	$18 \pm 2$	5
<i>silver</i>	1.3	$0.688 \pm 0.031$	19	$63^{+16}_{-14}$	1
<i>BEGe</i>	2.4	$0.720 \pm 0.018$	23	$42^{+10}_{-8}$	1
with PSD					
<i>golden</i>	17.9	$0.619^{+0.044}_{-0.070}$	45	$11 \pm 2$	2
<i>silver</i>	1.3	$0.619^{+0.044}_{-0.070}$	9	$30^{+11}_{-9}$	1
<i>BEGe</i>	2.4	$0.663 \pm 0.022$	3	$5^{+4}_{-3}$	0

<sup>†</sup>) in units of  $10^{-3} \text{ cts}/(\text{keV}\cdot\text{kg}\cdot\text{yr})$ .

Seven events are observed in the range  $Q_{\beta\beta} \pm 5 \text{ keV}$  before the PSD, to be compared to  $5.1 \pm 0.5$  expected background counts. No excess of events beyond the expected background is observed in any of the three data sets. This interpretation is strengthened by the pulse shape analysis. Of the six events from the semi-coaxial detectors, three are classified as SSE by ANN, consistent with the expectation. Five of the six events have the same classification by at least one other PSD method. The event in the BEGe data set is rejected by the A/E cut. No events remain within  $Q_{\beta\beta} \pm \sigma_E$  after PSD. All results quoted in the following are obtained with PSD.

To derive the signal strength  $N^{0\nu}$  and a frequentist coverage interval, a profile likelihood fit of the three data sets is performed. The fitted function consists of a constant term for the background and a Gaussian peak for the signal with mean at  $Q_{\beta\beta}$  and standard deviation  $\sigma_E$  according to the expected resolution. The fit has four free parameters: the backgrounds of the three data sets and  $1/T_{1/2}^{0\nu}$ , which relates to the peak integral by Eq. 1. The likelihood ratio is only evaluated for the physically allowed region  $T_{1/2}^{0\nu} > 0$ . It was verified that the method has always sufficient coverage. The systematic uncertainties due to the detector parameters, selection efficiency, energy resolution and energy scale are folded in with a Monte Carlo approach which takes correlations into ac-

TABLE II. List of all events within  $Q_{\beta\beta} \pm 5 \text{ keV}$

data set	detector	energy [keV]	date	PSD passed
<i>golden</i>	ANG 5	2041.8	18-Nov-2011 22:52	no
<i>silver</i>	ANG 5	2036.9	23-Jun-2012 23:02	yes
<i>golden</i>	RG 2	2041.3	16-Dec-2012 00:09	yes
<i>BEGe</i>	GD32B	2036.6	28-Dec-2012 09:50	no
<i>golden</i>	RG 1	2035.5	29-Jan-2013 03:35	yes
<i>golden</i>	ANG 3	2037.4	02-Mar-2013 08:08	no
<i>golden</i>	RG 1	2041.7	27-Apr-2013 22:21	no

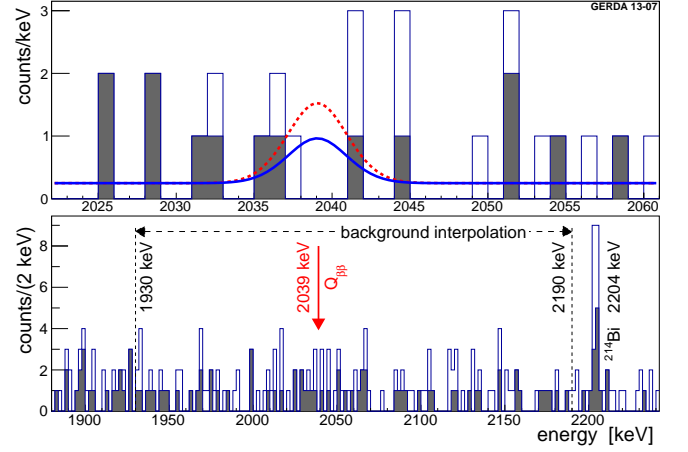


FIG. 1. The combined energy spectrum from all  $^{\text{enr}}\text{Ge}$  detectors without (with) PSD is shown by the open (filled) histogram. The lower panel shows the region used for the background interpolation. In the upper panel, the spectrum zoomed to  $Q_{\beta\beta}$  is superimposed with the expectations (with PSD selection) based on the central value of Ref. [11],  $T_{1/2}^{0\nu} = 1.19 \cdot 10^{25} \text{ yr}$  (red dashed) and with the 90 % upper limit derived in this work, corresponding to  $T_{1/2}^{0\nu} = 2.1 \cdot 10^{25} \text{ yr}$  (blue solid).

count. The best fit value is  $N^{0\nu} = 0$ , namely no excess of signal events above the background. The limit on the half-life is

$$T_{1/2}^{0\nu} > 2.1 \cdot 10^{25} \text{ yr} \quad (90 \% \text{ C.L.}) \quad (3)$$

including the systematic uncertainty. The limit on the half-life corresponds to  $N^{0\nu} < 3.5$  counts. The systematic uncertainties weaken the limit by about 1.5 %. Given the background levels and the efficiencies of Table I, the median sensitivity for the 90 % C.L. limit is  $2.4 \cdot 10^{25} \text{ yr}$ .

A Bayesian calculation [24] was also performed with the same fit described above. A flat prior distribution is taken for  $1/T_{1/2}^{0\nu}$  between 0 and  $10^{-24} \text{ yr}^{-1}$ . The toolkit BAT [25] is used to perform the combined analysis on the data sets and to extract the posterior distribution for  $T_{1/2}^{0\nu}$  after marginalization over all nuisance parameters. The best fit is again  $N^{0\nu} = 0$  and the 90 % credible interval is  $T_{1/2}^{0\nu} > 1.9 \cdot 10^{25} \text{ yr}$  (with folded systematic uncertainties). The corresponding median sensitivity is  $T_{1/2}^{0\nu} > 2.0 \cdot 10^{25} \text{ yr}$ .

## DISCUSSION

The GERDA data show no indication of a peak at  $Q_{\beta\beta}$ , i.e. the claim for the observation of  $0\nu\beta\beta$  decay in  $^{76}\text{Ge}$  is not supported. Taking  $T_{1/2}^{0\nu}$  from Ref. [11],  $5.9 \pm 1.4$  decays are expected (see note [26]) in  $\Delta E = \pm 2\sigma_E$  and  $2.0 \pm 0.3$  background events after the PSD cuts, as shown in Fig. 1. This can be compared with three events de-

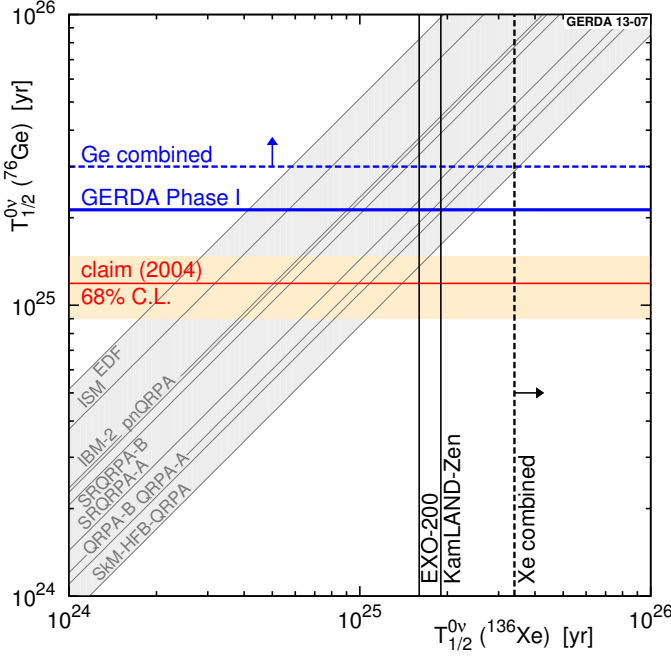


FIG. 2. Limits (90 % C.L.) on  $T_{1/2}^{0\nu}$  of  $^{76}\text{Ge}$  (this work) and  $^{136}\text{Xe}$  [14, 15] compared with the signal claim for  $^{76}\text{Ge}$  of Ref. [11] (68 % C.L. band). The lines in the shaded gray band are the predictions for the correlation of the half-lives in  $^{136}\text{Xe}$  and in  $^{76}\text{Ge}$  according to different NME calculations [27–33]. The selection of calculations and the labels are taken from Ref. [34].

tected, none of them within  $Q_{\beta\beta} \pm \sigma_E$ . The model ( $H_1$ ), which includes the claimed  $0\nu\beta\beta$  signal from Ref. [11], gives in fact a worse fit to the data than the background-only model ( $H_0$ ): the Bayes factor, namely the ratio of the probabilities of the two models, is  $P(H_1)/P(H_0) = 0.024$ . Assuming the model  $H_1$ , the probability to obtain  $N^{0\nu} = 0$  as the best fit from the profile likelihood analysis is  $P(N^{0\nu} = 0|H_1) = 0.01$ .

The GERDA result is consistent with the limits by HDM and IGEX. The profile likelihood fit is extended to include the energy spectra from HDM (interval 2000–2080 keV; Fig. 4 of Ref. [8]) and IGEX (interval 2020–2060 keV; Table II of Ref. [9]). Constant backgrounds for each of the five data sets and Gaussian peaks for the signal with common  $1/T_{1/2}^{0\nu}$  are assumed. Experimental parameters (exposure, energy resolution, efficiency factors) are obtained from the original references or, when not available, extrapolated from the values used in GERDA. The best fit yields  $N^{0\nu} = 0$  and a limit of

$$T_{1/2}^{0\nu} > 3.0 \cdot 10^{25} \text{ yr} \quad (90 \% \text{ C.L.}). \quad (4)$$

The Bayes factor is  $P(H_1)/P(H_0) = 2 \cdot 10^{-4}$ ; the claim is hence strongly disfavored.

Whereas only  $^{76}\text{Ge}$  experiments can test the claimed signal in a model-independent way, NME calculations can be used to compare the present  $^{76}\text{Ge}$  result to the recent

limits on the  $^{136}\text{Xe}$  half-life from KamLAND-Zen [14] and EXO-200 [15]. Fig. 2 shows the experimental results, the claimed signal (labeled “claim (2004)”) and the correlations for different predictions, assuming that the exchange of light Majorana neutrinos is the leading mechanism. Within this assumption, the present result can be also combined with the  $^{136}\text{Xe}$  experiments to scrutinize Ref. [11]. The most conservative exclusion is obtained by taking the smallest ratio  $M_{0\nu}(^{136}\text{Xe})/M_{0\nu}(^{76}\text{Ge}) \simeq 0.4$  [32, 33] of the calculations listed in Ref. [34]. This leads to an expected signal count of  $23.6 \pm 5.6$  ( $3.6 \pm 0.9$ ) for KamLAND-Zen (EXO-200). The comparison with the corresponding background-only models [35] yields a Bayes factor  $P(H_1)/P(H_0)$  of 0.40 for KamLAND-Zen and 0.23 for EXO-200. Including the GERDA result, the Bayes factor becomes 0.0022. Also in this case the claim is strongly excluded; for a larger ratio of NMEs the exclusion becomes even stronger. Note, however, that other theoretical approximations might lead to even smaller ratios and thus weaker exclusions.

The range for the upper limit on the effective electron neutrino mass  $m_{\beta\beta}$  is 0.2 - 0.4 eV. This limit is obtained by using the combined  $^{76}\text{Ge}$  limit of Eq. 4, the recently re-evaluated phase space factors of Ref. [36] and the NME calculations mentioned above [27–33]. Scaling due to different parameters  $g_A$  and  $r_A$  for NME is obeyed as discussed in Ref. [37].

In conclusion, due to the unprecedented low background counting rate and the good energy resolution intrinsic to HPGe detectors, GERDA establishes after only 21.6 kg·yr exposure the most stringent  $0\nu\beta\beta$  half-life limit for  $^{76}\text{Ge}$ . The long-standing claim for a  $0\nu\beta\beta$  signal in  $^{76}\text{Ge}$  is strongly disfavored, which calls for a further exploration of the degenerate Majorana mass scale. This will be pursued by GERDA Phase II aiming for a sensitivity increased by a factor of about 10.

## Acknowledgments

The GERDA experiment is supported financially by the German Federal Ministry for Education and Research (BMBF), the German Research Foundation (DFG) via the Excellence Cluster Universe, the Italian Istituto Nazionale di Fisica Nucleare (INFN), the Max Planck Society (MPG), the Polish National Science Centre (NCN), the Foundation for Polish Science (MPD programme), the Russian Foundation for Basic Research (RFBR), and the Swiss National Science Foundation (SNF). The institutions acknowledge also internal financial support.

The GERDA collaboration thanks the directors and the staff of the LNGS for their continuous strong support of the GERDA experiment.

- 
- <sup>a</sup> presently at: CEGEP St-Hyacinthe, Québec, Canada  
<sup>b</sup> presently at: INFN LNGS, Assergi, Italy  
<sup>c</sup> also at: Università di Firenze, Italy  
<sup>d</sup> also at: Moscow Inst. of Physics and Technology, Russia  
<sup>e</sup> also at: Int. Univ. for Nature, Society and Man, Dubna, Russia  
<sup>f</sup> presently at: Shanghai Jiaotong University, Shanghai, China  
<sup>g</sup> presently at: University North Carolina, Chapel Hill, USA  
<sup>h</sup> also at: Dipartimento di Science Fisica e Chimiche, University of L'Aquila, L'Aquila, Italy  
<sup>i</sup> Correspondence: gerda-eb@mpi-hd.mpg.de
- [1] A. S. Barabash, Phys. Rev. C **81**, 035501 (2010).
  - [2] V. I. Tretyak and Y. G. Zdesenko, At. Data Nucl. Data Tables **80**, 83 (2002).
  - [3] S. M. Bilenki and C. Giunti, Mod. Phys. Lett. A **27**, 1230015 (2012).
  - [4] J. D. Vergados, H. Ejiri, and F. Simkovic, Rept. Prog. Phys. **75**, 106301 (2012).
  - [5] W. Rodejohann, Int. J. Mod. Phys. E **20**, 1833 (2011).
  - [6] J. J. Gomez Cadenas *et al.*, Riv. Nuovo Cim. **35**, 29 (2012).
  - [7] B. J. Mount, M. Redshaw, and E. G. Myers, Phys. Rev. C **81**, 032501 (2010).
  - [8] H. V. Klapdor-Kleingrothaus *et al.* (Heidelberg-Moscow Collaboration), Eur. Phys. J. A **12**, 147 (2001).
  - [9] C. E. Aalseth *et al.* (IGEX Collaboration), Phys. Rev. D **65**, 092007 (2002).
  - [10] C. E. Aalseth *et al.* (IGEX Collaboration), Phys. Rev. D **70**, 078302 (2004).
  - [11] H. V. Klapdor-Kleingrothaus *et al.*, Phys. Lett. B **586**, 198 (2004).
  - [12] H. V. Klapdor-Kleingrothaus and I. Krivosheina, Mod. Phys. Lett. A **21**, 1547 (2006).
  - [13] B. Schwingenheuer, Ann. Phys. (Berlin) **525**, 269 (2013).
  - [14] A. Gando *et al.*, Phys. Rev. Lett. **110**, 062502 (2013).
  - [15] M. Auger *et al.*, Phys. Rev. Lett. **109**, 032505 (2012).
  - [16] K.-H. Ackermann *et al.* (GERDA Collaboration), Eur. Phys. J. C **73**, 2330 (2013).
  - [17] C. S. NV, Lammerdries 25, B-2439 Olen, Belgium.
  - [18] M. Agostini *et al.* (GERDA Collaboration), (2013), submitted to Eur. Phys. J. C, arXiv:1306.5084 [physics.ins-

- det].
- [19] M. Agostini *et al.*, J. Instrum. **6**, P08013 (2011).
  - [20] M. Agostini *et al.*, J. Phys.: Conf. Ser. **368**, 012047 (2012).
  - [21] D. Budjáš *et al.*, JINST **4**, P10007 (2009).
  - [22] M. Agostini *et al.*, JINST **6**, P03005 (2011).
  - [23] M. Agostini *et al.* (GERDA Collaboration), (2013), submitted to Eur. Phys. J. C, arXiv:1307.2610 [physics.ins-det].
  - [24] A. Caldwell and K. Kröninger, Phys. Rev. D **74**, 092003 (2006).
  - [25] A. Caldwell, D. Kollar, and K. Kröninger, Comput. Phys. Comm. **180**, 2197 (2009).
  - [26] The number of signal counts expected can be evaluated by rescaling the number of counts ( $28.75 \pm 6.86$ ) from Ref. [11] for the active exposure ( $f_{av} \cdot \mathcal{E}$ ). All other efficiency factors of Eq. (2) approximately cancel with the exception of  $\varepsilon_{psd}$ . The expected number of events after the PSD selection is 6.8 (6.5 in  $Q_{\beta\beta} \pm 2\sigma_E$ ). The difference with respect to the value calculated from  $T_{1/2}^{0\nu}$  is due to the efficiency factor  $\varepsilon_{fep}$ , which is taken to be 100 % in Ref. [11].
  - [27] T. R. Rodriguez and G. Martinez-Pinedo, Phys. Rev. Lett. **105**, 252503 (2010).
  - [28] J. Menendez *et al.*, Nucl. Phys. A **818**, 139 (2009).
  - [29] J. Barea, J. Kotila, and F. Iachello, Phys. Rev. C **87**, 014315 (2013).
  - [30] J. Suhonen and O. Civitarese, Nucl. Phys. A **847**, 207 (2010).
  - [31] A. Meroni, S. T. Petcov, and F. Simkovic, JHEP **1302**, 25 (2013).
  - [32] F. Simkovic, V. Rodin, A. Faessler, and P. Vogel, Phys. Rev. C **87**, 045501 (2013).
  - [33] M. T. Mustonen and J. Engel, (2013), arXiv:1301.6997 [nucl-th].
  - [34] P. S. Bhupal Dev *et al.*, (2013), arXiv:1305.0056 [hep-ph].
  - [35] The sensitivity of KamLAND-Zen corresponds to an equivalent background of  $460 \pm 21.5$  counts. The equivalent observed counts are  $-1.17\sigma$  lower, i.e. about 435 events [38]. EXO-200 expects  $7.5 \pm 0.7$  counts in the interval  $Q_{\beta\beta} \pm 2\sigma_E$  and observes 5 events.
  - [36] J. Kotila and F. Iachello, Phys. Rev. C **85**, 034316 (2012).
  - [37] A. Smolnikov and P. Grabmayr, Phys. Rev. C **81**, 028502 (2010).
  - [38] J. Bergström, JHEP **1302**, 093 (2013).